

Corrections Used when Measuring Materials Thermoelectric Properties by Harman Method

A. Abrutin¹, I. Drabkin², V. Osvenski³

¹ADV engineering, 109017, B. Tolmachevsky 5, Moscow, Russia, e-mail: adv_eng@aha.ru

² Institute of Chemical problems for Microelectronics, 109017, B. Tolmachevsky 5, Moscow, Russia, e-mail: igor@ng2449.spb.edu

³ State Institute of Rare Metals, 109017, B. Tolmachevsky 5, Moscow, Russia, e-mail: ottdel3@mail.girmet.ru

Abstracts

The Harman method is commonly used to determine thermoelectric properties of various materials. The main difficulty in applying the method is accounting for corrections related to electrical and thermal conductance of both current wires and probe wires, and to radiant losses from wires and from the sample. The paper contains solution of the set of one-dimension thermal conductivity equations describing thermal conditions in the sample and in the wires. On the basis of this solution the calculation of the sample thermoelectric properties made. In the original Harman method the current and probe wires thermal conductance is much less than that of the sample, minimizing adjustments for the thermal conductance of the wires. It results in the electrical resistance and Joule heat of the wires being greater than those of the sample. Calculations make it clear that corrections related to wires' Joule heat have a comparable value with the adjustments related to the wires conductance.

Introduction

The Harman Method is used both for tests of thermoelectric modules and for determination of thermoelectric properties of materials [1, 2, 3]. This method is especially suitable for acceptance tests of thermoelectric cooling modules.

In this paper we discuss the basic requirements to the Harman method for determination of thermoelectric properties of materials. It is accepted that the current I flowing through the sample with the Seebeck coefficient α and resistance R_s must be of such value that the Peltier heat Q_P on the side with temperature T ($Q_P = \alpha IT$) is far greater than the Joule heat $Q_J = I^2 R_s$. That is why

$$I \ll \frac{\alpha T}{R_s} = I_{max} \frac{T}{T_{0min}}, \quad (1)$$

where I_{max} is optimal current, T_{0min} is minimal temperature of the cold side. It is clear that inequality (1) is easily fulfilled and the temperature distribution along the sample is close to linear.

In order to diminish the influence of thermal conductance of the wire leads k_w on temperature pattern in the sample, k_w must be far less than the thermal conductance of the sample k_s . As the Wiedemann-Franz law demands that

$$R_w \gg n R_s, \quad (2)$$

where R_w is resistance of wire leads and n is some number in within the limits of 0,2 – 0,4 for usual thermoelectric materials. On the other hand, to achieve that the average temperature of the sample T_{av} be insignificantly differed from the ambient temperature T_a it is necessary that the Joule heat of the wire leads be far less than that of the sample, i.e.

$$R_w \ll R_s. \quad (3)$$

As (2) and (3) can't be satisfied simultaneously we assume that only inequality (2) is satisfied. In this case the sample is heated by the Joule heat of wire leads and not by that of the sample itself. As a consequence the current value must be much less than (1) and the estimations for it are:

$$I \ll (0.05 - 0.01) I_{max}. \quad (4)$$

To satisfy condition (4) is somewhat complicated in practice. That is why the wire leads always affect the measurement results and it is necessary to consider all factors more strictly when using the Harman method.

Corrections to the Harman method in one-dimension approach

Further we suppose that density of the current flow through the sample has constant value and therefore we can consider a one-dimension model. First of all we analyze the case when the wire leads are placed on both sides of the sample. For our consideration it is sufficient to use a 4-wires case because a bigger number of probe wires can be substituted by 4-wires with efficient values of thermal parameters. The measuring circuit can be seen on fig.1

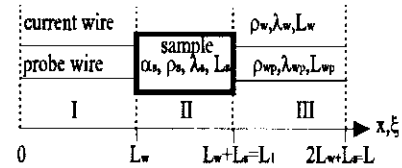


Fig.1. The sample with current and probe wires.

The coordinate x belongs to the current wires and the sample, the coordinate ξ - to the probe wires. The wires on both sides of the sample have the same length and diameter. Further we shall use symbols: α - the Seebeck coefficient, ρ - resistivity, λ - thermal conductivity, L - length, d - diameter, a - heat transfer coefficient, p - perimeter, T_0 - temperature of the cold side of the sample, T - temperature of the hot side of the sample. The lower index of the symbols explains to what these symbols are related: s - the sample, w - the current wire, wp - the probe wire.

In the area II and III (fig. 1) the heat transfer equations are

$$s_w \lambda_w \frac{d^2 T_w(x)}{dx^2} - a_w p_w (T_w(x) - T_a) + \frac{I^2 \rho_w}{s_w} = 0, \quad (5)$$

$$s_{wp} \lambda_{wp} \frac{d^2 T_{wp}(\xi)}{d\xi^2} - a_{wp} p_{wp} (T_{wp}(\xi) - T_a) = 0. \quad (6)$$

In the area II it is

$$s_s \lambda_s \frac{d^2 T_s(x)}{dx^2} - a_s p_s (T_s(x) - T_a) + \frac{I^2 \rho_s}{s_s} = 0. \quad (7)$$

The boundary conditions are:

$$T_w(0) = T_w(L_s + 2L_w) = T_{wp}(0) = T_{wp}(L_s + 2L_w) = T_a. \quad (8)$$

$$- \alpha T_s(L_w) + \lambda_s s_s \frac{dT_s(L_w)}{dx} - \lambda_w s_w \frac{dT_w(L_w)}{dx} -$$

$$- \lambda_{wp} s_{wp} \frac{dT_{wp}(L_w)}{d\xi} + a_w s_s (T_a - T_s(L_w)) = 0. \quad (9)$$

$$\alpha T_s(L_w + L) - \lambda_s s_s \frac{dT_s(L_w + L)}{dx} + \lambda_w s_w \frac{dT_w(L_w + L)}{dx} +$$

$$+ \lambda_{wp} s_{wp} \frac{dT_{wp}(L_w + L)}{d\xi} - a_w s_s (T_s(L_w + L) - T_a) = 0. \quad (10)$$

$$T_w(L_w) = T_s(L_w) = T_{wp}(L_w) \quad (11)$$

$$T_w(L_w + L_s) = T_s(L_w + L_s) = T_{wp}(L_w + L_s). \quad (12)$$

These conditions arise from the equality of temperature on the external sides of the wires to ambient temperature and from continuity of thermal fluxes and equality of temperatures on the boundaries of the sample and wires.

In I and III areas in equation (5) the substitution of the variable is made:

$$T_w = \vartheta_w(x) + T_a + \frac{I^2 \rho_w}{a_w p_w s_w}, \quad (13)$$

and in equation (6)

$$T_{wp} = \vartheta_{wp}(\xi) + T_a. \quad (14)$$

In area II in equation (7) substitution is used

$$T_s = \vartheta_s(x) + T_a + \frac{I^2 \rho_s}{a_s p_s s_s}. \quad (15)$$

Then equations (5) – (7) take the form:

$$\vartheta_w'' - b_w^2 \vartheta_w = 0, \quad x \in [0, L_w], [L_w + L_s, L_s + 2L_w], \quad (16)$$

$$\vartheta_{wp}'' - b_{wp}^2 \vartheta_{wp} = 0, \quad \xi \in [0, L_w], [L_w + L_s, L_s + 2L_w], \quad (17)$$

$$\vartheta_s'' - b_s^2 \vartheta_s = 0, \quad x \in [L_w, L_w + L_s], \quad (18)$$

where the following designations are used:

$$b_w^2 = \frac{a_w p_w}{\lambda_w s_w}, \quad b_{wp}^2 = \frac{a_{wp} p_{wp}}{\lambda_{wp} s_{wp}}, \quad b_s^2 = \frac{a_s p_s}{\lambda_s s_s}. \quad (19)$$

Solutions (16) – (18) are searched in the following expressions:

in area $x \in [0, L_w]$

$$\vartheta_w = C_1 sh(b_w x) + C_2 ch(b_w x), \quad (20)$$

in area $x \in [L_w, L_w + L_s]$

$$\vartheta_s = C_3 sh(b_s x) + C_4 ch(b_s x), \quad (21)$$

in area $x \in [L_w + L_s, L_s + 2L_w]$

$$\vartheta_w = C_5 sh(b_w x) + C_6 ch(b_w x), \quad (22)$$

for probe wires in area $\xi \in [0, L_w]$

$$\vartheta_{wp} = C_7 sh(b_{wp} \xi) + C_8 ch(b_{wp} \xi), \quad (23)$$

and in area $\xi \in [L_w + L_s, L_s + 2L_w]$

$$\vartheta_{wp} = C_9 sh(b_{wp} \xi) + C_{10} ch(b_{wp} \xi), \quad (24)$$

where $C_1 - C_{10}$ are constants of integrity, which are deduced from boundary conditions (8) – (12). It results in equations, which can be solved in a numerical form. These equations are given in Appendix 1, where the following designations are used:

$$\alpha^+ = \alpha l + a_s s_s, \quad \alpha^- = \alpha l - a_s s_s, \quad (25)$$

$$\lambda_w s_w b_w = \beta_w, \quad \lambda_s s_s b_s = \beta_s, \quad L_w + L_s = L_1, \quad 2L_w + L_s = L, \quad (26)$$

$$R = \frac{\rho_s}{a_s p_s s_s} - \frac{\rho_w}{a_w p_w s_w}. \quad (27)$$

Average temperature of the sample \bar{T} equals:

$$\bar{T}_s = T_a + \frac{I^2 \rho_s}{a_s p_s s_s} + \frac{2}{L_s b_s} \cdot$$

$$\left[C_3 sh\left(b_s \left(L_w + \frac{L_s}{2}\right)\right) sh\left(b_s \frac{L_s}{2}\right) + C_4 ch\left(b_s \left(L_w + \frac{L_s}{2}\right)\right) sh\left(b_s \frac{L_s}{2}\right) \right] \quad (28)$$

Temperature difference for both sides of the sample equals:

$$\Delta T_s = 2C_3 ch\left(b_s \left(L_w + \frac{L_s}{2}\right)\right) sh\left(b_s \frac{L_s}{2}\right) +$$

$$+ 2C_4 sh\left(b_s \left(L_w + \frac{L_s}{2}\right)\right) sh\left(b_s \frac{L_s}{2}\right). \quad (29)$$

In the similar way we can find temperature distribution along the sample when two wires method (Fig.2) is used.

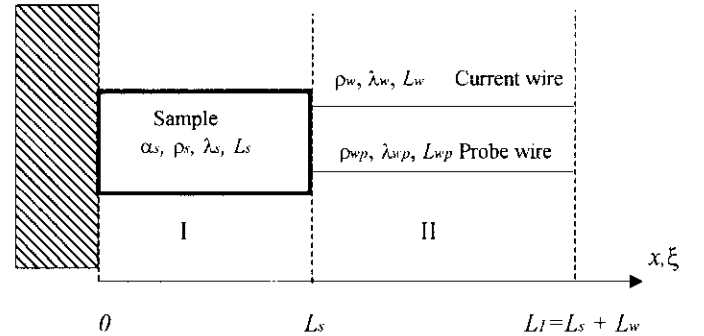


Fig. 2. General two wires circuit for the Harman method.

In this case the temperature distribution along the sample and the wires has following form:

$$T_s = T_a + \frac{I^2 \rho_s}{a_s p_s s_s} + C_{11} sh(b_s x) + C_{12} ch(b_s x), \quad (30)$$

$$T_w = T_a + \frac{I^2 \rho_w}{a_w p_w s_w} + C_{13} sh(b_w x) + C_{14} ch(b_w x), \quad (31)$$

$$T_{wp} = T_a + C_{15} sh(b_{wp} x) + C_{16} ch(b_{wp} x), \quad (21), \quad (32)$$

where constants $C_{11} - C_{16}$ are found from the numerical solution of the linear system given in Appendix 2.

The average temperature of the sample is

$$\bar{T}_s = T_a + \frac{I^2 \rho_s}{a_s p_s s_s} + \frac{1}{L_s b_s} (C_{11} ch(b_s L_s) + C_{12} sh(b_s L_s) - 1), \quad (33)$$

and the temperature difference on the sample is

$$\Delta T_s = C_{11} sh(b_s L_s) + C_{12} (ch(b_s L_s) - 1). \quad (34)$$

The Results of Numerical Calculations

The numerical calculations are made for a thermoelectric material sample in the form of a parallelepiped with $4 \times 4 \times 10 \text{ mm}^3$ dimensions. Length of the current and probe wires is 30 mm. Temperature distribution along the current wires and the sample is given in fig. 3. Calculations made for the sample properties: $\lambda_s = 1.4 \text{ W/mK}$, $\sigma_s = 1000 \text{ } \Omega^{-1} \text{ cm}^{-1}$, $\alpha_s = 200 \text{ } \mu\text{V/K}$, $Z = 2.86 \cdot 10^{-3} \text{ K}^{-1}$, $I_{\max} = 7.3 \text{ A}$. Diameters of the current and probe wires are the same - 0.1 mm. Ambient temperature is 293 K.

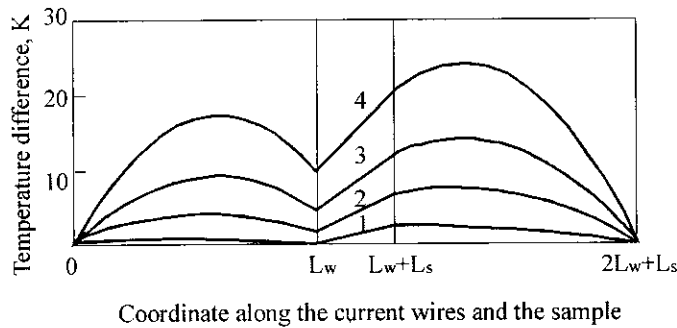


Fig. 3. Temperature distribution along the current wires and the sample for different currents flowing through the sample: 1 - 0.1 A = 0.014 I_{\max} , 2 - 0.2 A = 0.027 I_{\max} , 3 - 0.3 A = 0.041 I_{\max} , 4 - 0.4 A = 0.055 I_{\max} .

It is clear from fig. 3 that for usual currents the temperatures both for the heat absorbing side and for the heat emitting side are higher than the ambient temperature. The reason of it is that the thermal fluxes caused by the Peltier heat on both sides of the sample are smaller than thermal fluxes from the current wires.

We denote the sample voltage as $U = U_\alpha + U_r$, where $U_\alpha = \alpha \Delta T_s$ and $U_r = I R_s$. The results of the calculation of \bar{T}_s , ΔT_s , $Z_{\text{eff}} = U_\alpha / U_r \bar{T}_s$ are given in Table 1.

Table 1. The dependence of calculated parameters on current

Current, A	0.1	0.2	0.3	0.4	0.5	0.6
$\bar{T}_s, \text{ K}$	293.6	295.3	298.1	302.1	307.2	313.7
$\Delta T_s, \text{ K}$	2.42	4.86	7.37	9.95	12.65	15.50
$Z_{\text{eff}} 10^3, \text{ K}^{-1}$	2.64	2.64	2.64	2.64	2.64	2.64

The processing of the experimental results is done in the following way. In zero approximation it is accepted that the value of the thermal conductivity is usual for the measured sample. After it the set of equations given in Appendix 1 or 2 is solved and constants of integrity are found for different sample emissivity. The value of the sample emissivity is taken from the condition of equality of the average sample temperatures, which are calculated and obtained

This table shows that Z_{eff} is always smaller than Z of the thermoelectric material and has weak dependence on the sample current. Because of it a transfer multiplier, which is defined for the given measuring cell can be used in wide interval of current values. For example, in the considered case the transfer multiplier is 1.087. This value is bigger than the correcting multiplier due to thermal conductance of the wire leads. This correcting multiplier, as it is easy to show, equals

$$1 + \frac{\lambda_w (s_w + s_{wp}) L_s}{2 L_w \lambda_s s_s}$$

equals for the considered case to 1.047.

If the dimensions and parameters of the sample, and the wires are defined and the current is given, then the average temperature of the sample depends mainly on the emissivity of the sample for the vacuum measurements. Under these conditions the temperature difference between the opposite sides of the sample is defined only by the thermal conductivity of the sample. The dependence of $\Delta \bar{T}$ on thermal conductivity is clear from fig. 4.

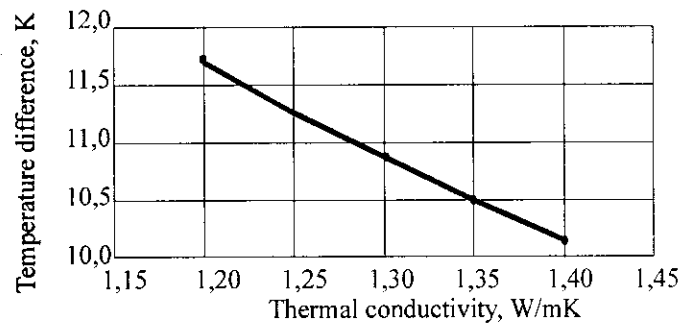


Fig. 4. The calculated dependence of the temperature difference between the opposite sides of the sample.

The above-mentioned facts show how to process the experimental results of the measurement made according to the Harman method. No doubt the new method is more complicated than the usual Harman method because the results of ZT measurements depend in a complex way on the thermoelectric parameters. However, the algorithm of the processing is simple enough and convenient. The sample electrical resistance is defined by measuring U_r with alternate current. It is evident that U_r must be measured for the same average temperature as it is done in measuring U_α . As the sample heating is made mainly by the wires Joule heat the change of alternate current to direct one with the same values causes small change in the average temperature of the sample, as it is shown by the calculations. The Seebeck coefficient is defined from measurements in a different cell or in the same cell, but with additional thermocouple wires connected to the opposite sides of the sample (6-wires measuring circuit).

experimentally. The next step is defining the new value of thermal conductivity from the condition of equality of the calculated and experimental values of ΔT . The new value of thermal conductivity is used for calculation of the new value of emissivity and so on. This procedure converges very quickly, so few approximations are sufficient.

It is clear that if the sample has inhomogeneities then the measuring results may be distorted. The influence of

transverse inhomogeneities with characteristic dimensions which are less than the sample length is discussed everywhere [4] and it is known that such inhomogeneities lead to diminishing the value of Z . Another type of inhomogeneities that can affect the value of Z is longitudinal inhomogeneity of the charge carrier concentration with characteristic dimensions of order or larger than the sample length (for example, inhomogeneities of the composition of the grown crystal). This inhomogeneity leads to the longitudinal gradient of the Seebeck coefficient and also to emission or absorption of the Thomson heat depending on the direction of the current. If this gradient does not change the sign then the measured value ΔT depends on the direction of the current. This gives dependence of the measured Seebeck coefficient and Z on the current direction. If the gradient of the charge carriers changes the sign then in case when the middle part of the sample has a larger concentration of charge carriers than that on the sides then the measured Z is larger than the real Z of every part of the sample (because seeming growth of electrical conductance). In the opposite case the result of measuring the value of Z is also opposite. Such influence of inhomogeneities on measured properties must be taken into account and manifestations of it must not be left without attention.

Experimental Investigations

The measuring unit for Z of thermoelectrics was designed and calculating computer program was made up. The measuring cell is given on fig. 5.

This cell can measure 3 samples simultaneously. Measurements were fulfilled in vacuum $2 - 3 \cdot 10^{-5}$ Torr. The numerous measurements of thermoelectrics on the base Bi_2Te_3 was made with this unit. The emissivity for $\text{Bi}_{0.5}\text{Sb}_{1.5}\text{Te}_3$ was $0.58 - 0.78$ and for $\text{Bi}_2\text{Te}_{2.7}\text{Se}_{0.3}$ – $0.55 - 0.70$. The ratio Z/Z_{eff} was 1.100 ± 0.005 .

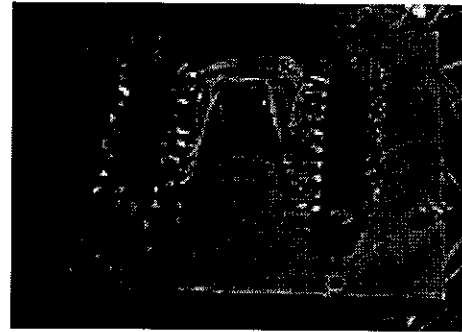


Fig.5. The measuring cell.

Conclusion

Modification of the Harman method proposed for measuring Z of thermoelectric materials, based on the solution of thermal equation in one-dimension approximation. This method makes it possible to consider the thermal emission of the sample and thermal fluxes along the current and probe wires. It has been shown that the Joule heat in current wires makes considerable contribution to the correction of the true value of Z . The algorithm of processing of the experimental results has also been proposed.

References

1. Harman T.C, Honig J.M. J. Appl. Phys. 'Special techniques for measurement of thermoelectric properties', J. Appl. Phys, **29**, p1373, (1959).
2. Buist R.J.. Proc.XI Int. Conf. on Thermoelectrics. Arlington. (1992).
3. Gromov G, Ershova L. "Z-meter: Easy-to-use Application and Theory. Proc. VI European Workshop on Thermoelectrics, Freiburg, September, 2001.
4. B.M. Goltsman, V.A. Kudinov, V.A. Smirnov. Semiconductor thermoelectric materials on the base Bi_2Te_3 , Moscow, 1972

Appendix 1

0	1	0	0	0	0	1	0	0	0
0	0	0	0	$sh(b_w L)$	0	0	0	0	$sh(b_w L)$
$-sh(b_w L_w)$	$-ch(b_w L_w)$	$sh(b_s L_w)$	$ch(b_s L_w)$	0	$-sh(b_w L_w)$	$-ch(b_w L_w)$	$sh(b_s L_w)$	$ch(b_s L_w)$	0
0	0	$sh(b_s L_l)$	$ch(b_s L_l)$	$-sh(b_w L_l)$	0	0	$sh(b_s L_l)$	$ch(b_s L_l)$	$-sh(b_w L_l)$
$-\beta_w ch(b_w L_w)$	$-\beta_w sh(b_w L_w)$	$-\alpha^+ sh(b_s L_w) + \beta_s ch(b_s L_w)$	$-\alpha^+ ch(b_s L_w) + \beta_s sh(b_s L_w)$	0	$-\beta_w ch(b_w L_w)$	$-\beta_w sh(b_w L_w)$	$-\alpha^+ sh(b_s L_w) + \beta_s ch(b_s L_w)$	$-\alpha^+ ch(b_s L_w) + \beta_s sh(b_s L_w)$	0
0	0	$\alpha^- sh(b_s L_l) - \beta_s ch(b_s L_l)$	$\alpha^- ch(b_s L_l) - \beta_s sh(b_s L_l)$	$\beta_w ch(b_w L_l)$	0	0	$\alpha^- sh(b_s L_l) - \beta_s ch(b_s L_l)$	$\alpha^- ch(b_s L_l) - \beta_s sh(b_s L_l)$	$\beta_w ch(b_w L_l)$
0	0	0	0	0	0	0	0	0	0
0	0	0	0	0	0	0	0	0	0
0	0	$-sh(b_s L_w)$	$-ch(b_s L_w)$	0	0	0	$-sh(b_s L_w)$	$-ch(b_s L_w)$	0
0	0	$-sh(b_s L_l)$	$-ch(b_s L_l)$	0	0	0	$-sh(b_s L_l)$	$-ch(b_s L_l)$	0

$$\begin{pmatrix} C_1 \\ C_2 \\ C_3 \\ C_4 \\ C_5 \\ C_6 \\ C_7 \\ C_8 \\ C_9 \\ C_{10} \end{pmatrix} = \begin{pmatrix} -\frac{I^2 \rho_w}{a_w p_w s_w} \\ \frac{I^2 \rho_w}{a_w p_w s_w} \\ -I^2 R \\ -I^2 R \\ \alpha T_a + \frac{\alpha^+ I^2 \rho_s}{a_s p_s s_s} \\ -\alpha T_a - \frac{\alpha^- I^2 \rho_s}{a_s p_s s_s} \\ 0 \\ 0 \\ \frac{I^2 \rho_s}{a_s p_s s_s} \\ \frac{I^2 \rho_s}{a_s p_s s_s} \end{pmatrix}$$

Appendix 2

0	1	0	0	0	0	=	$\begin{pmatrix} \frac{I^2 \rho_s}{a_s p_s s_s} \\ \frac{I^2 \rho_w}{a_w p_w s_w} \\ 0 \\ -I^2 R \\ \frac{I^2 \rho_s}{a_s p_s s_s} \\ -\alpha T_a - \alpha^- \frac{I^2 \rho_s}{a_s p_s s_s} \end{pmatrix}$	$\begin{pmatrix} C_{11} \\ C_{12} \\ C_{13} \\ C_{14} \\ C_{15} \\ C_{16} \end{pmatrix}$
0	0	$sh(b_w L_l)$	$ch(b_w L_l)$	0	0			
0	0	0	0	$sh(b_{wp} L_l)$	$ch(b_{wp} L_l)$			
$sh(b_s L_s)$	$ch(b_s L_s)$	$-sh(b_w L_s)$	$-ch(b_w L_s)$	0	0			
$sh(b_s L_s)$	$ch(b_s L_s)$	0	0	$-sh(b_{wp} L_s)$	$-ch(b_{wp} L_s)$			
$\alpha^- sh(b_s L_s) - \beta_s ch(b_s L_s)$	$\alpha^- ch(b_s L_s) + \beta_s sh(b_s L_s)$	$\beta_w ch(b_w L_s)$	$-\beta_w sh(b_w L_s)$	$\beta_{wp} ch(b_{wp} L_s)$	$\beta_{wp} sh(b_{wp} L_s)$			